PROCEEDINGS of the
23rd International Congress on Acoustics

9 to 13 September 2019 in Aachen, Germany

Analytical and computational modeling of viscothermal acoustic damping in perforated microstructures

Vahid NADERYAN[1]; Richard RASPET; Craig HICKEY; Mohammad MOHAMMADI

National Center for Physical Acoustics, University of Mississippi, USA

ABSTRACT

Predicting the viscothermal acoustic behavior of microstructures is crucial in the design of micro-electro-mechanical systems (MEMS). In MEMS structures the dimensionless shear wave-number is typically smaller than one. Therefore, the viscous effects are larger than inertial effects and are the dominant part of the impedance. In this work, an analytical solution for the viscothermal acoustic impedance for perforated microstructures used in MEMS devices is developed based on the low reduced-frequency (LRF) method. This solution is based on a full-plate approach, as opposed to the single-cell approach, which includes all viscous and thermal losses as well as compressibility and inertial effects. Additionally, a 3D viscothermal acoustic model using the finite element method (FEM) is developed to solve the problem numerically for the case of a MEMS microphone. The results of the analytical LRF solution are in good agreement with the FEM results. The results can be applied in designing MEMS devices to minimize the damping and to optimize the acoustic performance of the MEMS devices.

Keywords: MEMS, Squeeze-film damping, Viscothermal acoustics

1. INTRODUCTION

MEMS are micro-dimensional devices and elements that are made using modern micro-fabrication techniques. In many MEMS devices (e.g. microphones), a diaphragm moves relative to a stationary back-plate to form a parallel-plate capacitor. Since the gap spacing between the plates is very small compared to the lateral dimensions, a thin film of air will be squeezed when the diaphragm is oscillating. This results in a complex pressure distribution between the plates that acts as damping and spring forces. This phenomenon called squeeze-film damping is typically the dominant source of internal thermal-mechanical noise in MEMS (1). According to the fluctuation-dissipation theorem, the noise spectral level is proportional to visco-thermal damping in the system (2).

Simulation tools are necessary for modeling the behavior of MEMS devices for designers and developers to advance the technology to the next levels. Evaluation of the squeeze-film and other viscous and thermal losses of MEMS devices is a crucial and challenging task which requires studying the behavior of the fluid and its reaction to the diaphragm's motion. Several analytical models for squeeze-film damping and spring effects have been developed over the past decades. Most of these models are derived starting from the well-known Reynolds equation (3). In order to improve the accuracy of the prediction of damping in modern MEMS devices, several geometric or flow conditions are typically added to the basic models. Modeling the effect of the perforations in the back-plates is the most significant one and has been the center of attention in most of the recent works. Other secondary effects include compressibility, inertia, gas rarefaction, the end effects of the holes, and edge (border) of the plate effects.

Typically, in many MEMS devices (such as microphones, accelerometers, etc.) perforations are introduced into one of the parallel plates to reduce the squeeze-film damping. These perforations also facilitate the etch release of the sacrificial layer between the plates. By means of the perforations, the air flow can move through the holes and consequently, the squeeze-film damping is reduced, however, extra damping due to the motion of the air through the holes is added to the system. Therefore, modeling the squeeze-film effect for perforated MEMS plates is complex, challenging, and important.

Studies on the modeling of perforated MEMS can be subdivided into two categories based on the approach used: single-cell approach and full-plate approach. The models consider a uniformly

[1] Vahid.nad@gmail.com

distributed pattern of holes on the plate. Each hole is surrounded by a cell. In the single-cell approach, the squeeze-film damping of a single-cell is calculated from the Reynolds equation and the proper boundary conditions for a cell. Then the damping of the entire plate is calculated by multiplying the result by the total number of the cells in the plate. Many of the studies in the literature have used the single-cell approach, such as references (4-10).

In the full-plate approach, the Reynolds equation is modified for the flow in the gap and through the perforations. The modified Reynolds equation is then solved with the boundary conditions of the plate border to calculate the total damping of the plates. Most of the existing solutions are provided for rectangular plates. In rectangular MEMS two edges are usually clamped represented by a no-flow wall boundary condition and two edges are open requiring an open venting boundary condition. Although there are very limited numbers of existing solutions for circular MEMS, circular MEMS are also very common, specifically in microphones. Several previous studies such as references (11-15) have followed the full-plate approach to model the perforated MEMS by solving the modified Reynolds equation for different plate geometries and boundary conditions.

In this work, a full-plate approach will be followed to model the losses in MEMS structures. All the full-plate solutions in the literature are based on the modified Reynolds equation based on the lubrication approximation. In the lubrication approximation, the Navier-Stoke equation is integrated over the separation distance between the plane surfaces to derive the Reynolds equation, therefore, it is valid for sufficiently small gaps. For perforated micro-plates, the flow domain is not narrow in the region of the holes. Hence, the Reynolds equation is not valid unless the pitch of the holes is much larger than the gap and the diameter of the holes, which is not the case in many devices (10).

Better theory and calculations will lead to better understanding and better agreement with real devices. In this work, pressure and velocity fields in the gap region and the hole region will be derived using the low-reduced frequency (LRF) method that is valid for devices with small transverse dimensions with respect to a wavelength. A new physical full-plate solution including thermal and viscous losses as well as inertial and compressibility effects will be developed using the proper boundary conditions. A 3D finite element model is also developed in order to validate the analytical model. The proposed model will be applicable to various geometries and boundary conditions.

2. LOW REDUCED-FREQUENCY SOLUTION FOR MEMS

2.1 Low Reduced-Frequency Method

In this work, a solution using the LRF method will be developed based on the full-plate approach. Tijdeman (16) introduced dimensionless parameters to develop a model for viscothermal sound propagation in cylindrical pores when the dimensions are small with respect to a wavelength. The LRF solution is based on five fundamental equations that describe the motion of fluids in circular cylinders: the Navier-Stokes equations in both axial and radial directions, the equation of continuity, the equation of state, and the entropy equation. In the LRF model, the system of equations is rewritten in such a way that equations describing the fluid along the propagation direction are decoupled from the equations governing cross-sectional behavior. The LRF method is a good method for full analysis of MEMS devices which includes all viscous and thermal losses as well as compressibility and inertial effects.

2.2 Viscothermal Solution for MEMS

2.2.1 LRF Solution for Parallel Plates

In order to utilize the LRF method to solve for the damping and spring forces in the parallel-plate MEMS the following dimensionless parameters are defined which are reduced-frequency, axial variable, radial variable, shear wave-number, and thermal wave-number, respectively:

$$\Omega = \omega g_0 / c_0 \tag{1}$$

$$\xi = z / g_0 \tag{2}$$

$$\eta = \omega r / c_0 \tag{3}$$

$$\lambda = g_0 \sqrt{\rho_0 \omega / \mu} \tag{4}$$

$$\lambda_T = g_0 \sqrt{\rho_0 c_p \omega / \kappa} \tag{5}$$

where ω is the angular frequency, g_0 is the gap spacing, c_0 is the velocity of sound, ρ_0 is the density of air, μ is the viscosity, c_p is the specific heat at constant pressure, and κ is the thermal conductivity. The principle approximation of this method is to require that the reduced-frequency be small ($\Omega \ll 1$). Figure 1 shows a schematic top view of a perforated micro-plate. A cross-section view is displayed in Figure 2 to show the parameters and the coordinate system.

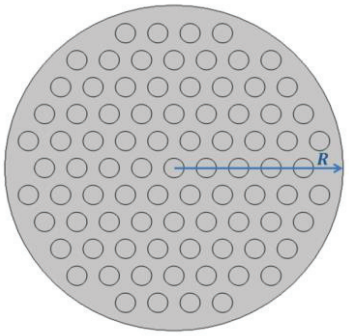

Figure 1 – Schematic top view of a perforated micro-plate.

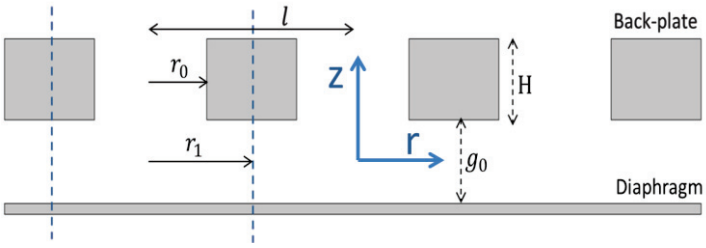

Figure 2 – Cross-section view of a perforated MEMS and the coordinate system.

The dimensionless equations are linearized and isothermal boundary condition is applied on the top and bottom plates ($\xi = \pm 1/2$). With a velocity boundary condition for the diaphragm and an impedance boundary condition for the fixed back-plate and venting boundary condition at the plate border, after algebraic manipulations the damping coefficient, D, and the spring coefficient, S, are calculated:

$$D + iS = \frac{i\gamma\pi R^2 p_0}{\omega g_0 f(\lambda) C}\left[1 - \frac{2c_0}{\sqrt{C}\omega R}\frac{J_1\left(\sqrt{C}\frac{\omega R}{c_0}\right)}{J_0\left(\sqrt{C}\frac{\omega R}{c_0}\right)}\right] \tag{6}$$

where γ is the ratio of specific heats, R is the plate radius, p_0 is the ambient pressure, J_0 and J_1 are zeroth order and first order Bessel functions of the first kind, respectively, and we have defined:

$$C = B - i/\Omega f(\lambda) Z \tag{7}$$

$$B = \gamma - (\gamma - 1) f(\lambda_T)/f(\lambda) \tag{8}$$

$$f(\lambda) = 1 - 2\sin(\sqrt{i}\,\lambda/2)/\sqrt{i}\lambda\cos(\sqrt{i}\,\lambda/2) \tag{9}$$

where Z is the dimensionless specific acoustic impedance of the perforated back-plate which will be calculated in the next sub-section. The expression of Equation 6 is the principal result of this work that contains all relevant physics.

2.2.2 Impedance of the Perforated Back-plate

The impedance of the perforated back-plate consists of two parts: the impedance of the holes, Z_h, and the impedance of the squeeze-film in the gap between two plates, Z_g.

$$Z = Z_h + Z_g \tag{10}$$

In order to find the impedance of the holes, Z_h, we use Tijdeman's LRF solution for the flow inside a cylindrical tube with zero velocity boundary condition at the walls of the tubes. After algebraic

manipulations the dimensionless specific acoustic impedance of the perforated plate is:

$$Z_h = \frac{Z_{int}}{\sigma}\left[\frac{\rho_0 c_0 \,\mathrm{Cos}(kH) - iZ_{int}\,\mathrm{Sin}(kH)}{Z_{int}\,\mathrm{Cos}(kH) - i\rho_0 c_0\,\mathrm{Sin}(kH)}\right] - 1 \tag{11}$$

where

$$k = (\omega/c_0)\sqrt{B} \tag{12}$$

$$Z_{int} = 1/\left(f(\lambda)\sqrt{B}\right) \tag{13}$$

where σ is the porosity and H is the plate thickness. This solution assumes a plate with an infinite thickness which does not include the end effects of the tube. However, for plates with finite thickness, the effect of the ends of the tube has to be taken into account. The end length corrections for the imaginary part (l_{ei}) and real part (l_{er}) of the impedance are (17):

$$l_{ei} = (16r_0/3\pi)(1 - \sqrt{\sigma}) \tag{14}$$

$$l_{er} = 0.94r_0 \tag{15}$$

where r_0 is the radius of the holes.

The impedance of the gap region using the LRF method is solved to be:

$$Z_g = \frac{i}{\Omega f(\lambda) B}\left[\frac{2r_0 c_0}{\sqrt{B}\omega({r_1}^2 - {r_0}^2)}\alpha - 1\right] \tag{16}$$

where r_0 is the equivalent radius of a cell and

$$\alpha = \frac{Y_1\left(\sqrt{B}\frac{\omega r_1}{c_0}\right)J_1\left(\sqrt{B}\frac{\omega r_0}{c_0}\right) - J_1\left(\sqrt{B}\frac{\omega r_1}{c_0}\right)Y_1\left(\sqrt{B}\frac{\omega r_0}{c_0}\right)}{Y_0\left(\sqrt{B}\frac{\omega r_0}{c_0}\right)J_1\left(\sqrt{B}\frac{\omega r_1}{c_0}\right) - J_0\left(\sqrt{B}\frac{\omega r_0}{c_0}\right)Y_1\left(\sqrt{B}\frac{\omega r_1}{c_0}\right)} \tag{17}$$

where Y_0 and Y_1 are zeroth order and first order Bessel functions of the second kind, respectively.

3. Finite Element Method

In this section, the Finite Element Method (FEM) simulations are conducted to compare with the results of the analytical model. This is achieved by solving the linearized Navier-Stokes equations, momentum equation, continuity equation, and energy equation in the Thermoviscous Acoustics (TA) interfaces in the Acoustics Module of COMSOL® software. Both the viscous and heat conduction effects are included in this interface and it solves for the acoustic perturbations in pressure, velocity, and temperature.

The solution for circular MEMS is solved using a 3D COMSOL® model. Due to the symmetric pattern of the holes on the back-plate a 30-degree pie section of the MEMS is modeled and symmetry boundary condition is used at the edges. The isothermal no-slip wall boundary condition is applied on the back-plate walls. The diaphragm is driven with a constant harmonic vertical velocity. Open venting boundary condition is applied at the circular perimeter of the plate. The real and imaginary parts of the force exerted on the surface of the diaphragm divided by its velocity represent the damping and spring force coefficients, respectively. Figure 3 displays cross-sections of the velocity field in the MEMS at $1kHz$.

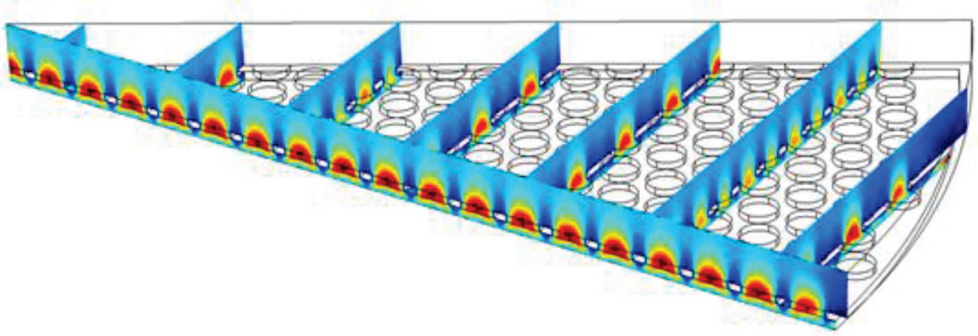

Figure 3 – Velocity field cross-sections at 1kHz.

4. RESULTS

In this section the damping force coefficient calculated from the LRF method, Equation 6, is compared with the FEM results and with two former theoretical models in the literature. The Li (15) model is based on the full-plate approach for a circular MEMS, and the Homentcovschi & Miles (10) model is based on the single-cell approach. Figure 4 shows the damping force coefficient as a function of pitch. Pitch (l) is defined as the distance between the centers of the neighboring holes, as displayed in Figure 2. The parameters of Table 1 are used for the calculations.

Table 1 - MEMS parameters used in the calculations

$R\ (\mu m)$	$g_0(\mu m)$	$\sigma\ (\%)$	$H\ (\mu m)$	*Frequency (Hz)*
400	4	50	3	1000

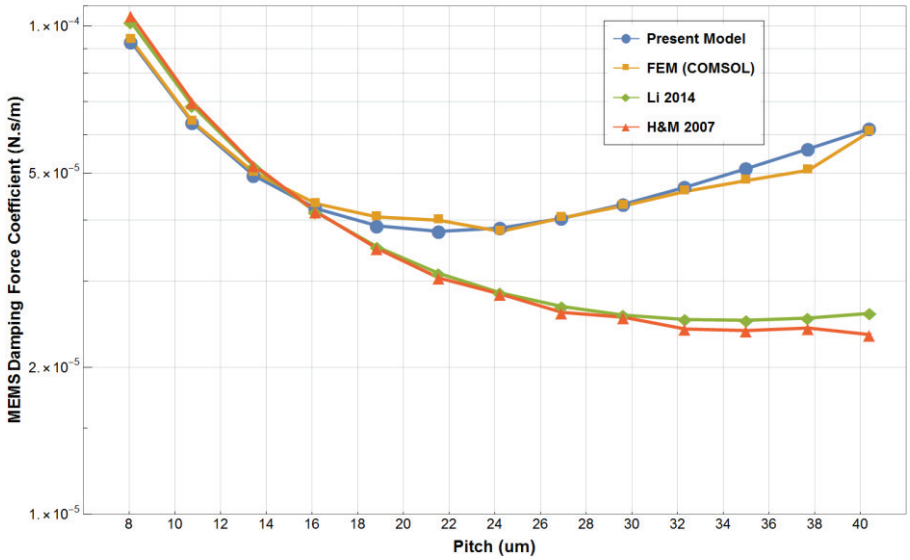

Figure 4 – MEMS damping force coefficient.

The present model is in a better agreement with the FEM results compared to the previous models, especially at higher pitch values. At lower pitch values (smaller holes) the damping through the holes is dominant, but at higher pitch values (larger holes) the gap damping is dominant. The total damping is a combination of these two. This is the reason that there exists an optimum pitch value. This suggests that at a fixed porosity and for a set of given MEMS parameters, an optimum pitch value can be calculated that minimizes the total damping. For the example of Figure 4, the optimum pitch value is around 22 μm.

5. CONCLUSIONS

Accurate physical models are crucial for the study of the MEMS devices. Such models can guide the designers and developers to advance the performance of such devices. In this work, the LRF method is utilized to develop a new physical model for the viscothermal acoustic mechanism in parallel-plate perforated MEMS. This model is based on a full-plate approach and includes thermal and viscous losses as well as inertial and compressibility effects.

Comparison of the model with the 3D viscothermal acoustic FEM results shows a good agreement compared with the previous models in the literature. The results suggest that the pitch of the perforations can be optimized in order to minimize the damping of the MEMS. The accuracy of this physical model leads to a better understanding of the phenomena and better agreement with real devices. The proposed model is applicable to various geometries and boundary conditions.

ACKNOWLEDGMENTS

We acknowledge Knowles Corporation for their support of this work.

REFERENCES

1. Kuntzman ML, LoPresti JL, Du Y, Conklin WF, Naderyan V, Lee SB, Schafer D, Pedersen M, Loeppert PV. Thermal boundary layer limitations on the performance of micromachined microphones. The Journal of the Acoustical Society of America, 144(5), 2838-2846; 2018.
2. Gabrielson TB. Mechanical-thermal noise in micromachined acoustic and vibration sensors. IEEE transactions on Electron Devices, 40(5), 903-909; 1993.
3. Mohammad IY. MEMS Linear and Nonlinear Statics and Dynamics. Springer, New York; 2011.
4. Škvor Z. On the acoustical resistance due to viscous losses in the air gap of electrostatic transducers. Acta acustica united with acustica, 19(5), 295-299; 1967.
5. Bao M, Yang H, Sun Y, Wang Y. Squeeze-film air damping of thick hole-plate. Sensors and Actuators A: Physical, 108(1-3), 212-217; 2003.
6. Kwok PY, Weinberg MS, Breuer KS. Fluid effects in vibrating micromachined structures. Journal of Microelectromechanical systems, 14(4), 770-781; 2005.
7. Mohite SS, Sonti VR, Pratap R. A compact squeeze-film model including inertia, compressibility, and rarefaction effects for perforated 3-D MEMS structures. Journal of Microelectromechanical systems, 17(3), 709-723; 2008.
8. Veijola T. Analytic damping model for an MEM perforation cell. Microfluidics and Nanofluidics, 2(3), 249-260; 2006.
9. Homentcovschi D, Miles RN. Analytical model for viscous damping and the spring force for perforated planar microstructures acting at both audible and ultrasonic frequencies. The Journal of the Acoustical Society of America, 124(1), 175-181; 2008.
10. Homentcovschi D, Miles RN. Viscous damping and spring force in periodic perforated planar microstructures when the Reynolds' equation cannot be applied. The Journal of the Acoustical Society of America, 127(3), 1288-1299; 2010.
11. Bao M, Yang H, Sun Y, French PJ. Modified Reynolds' equation and analytical analysis of squeeze-film air damping of perforated structures. Journal of Micromechanics and Microengineering, 13(6), 795; 2003.
12. Bao M, Yang H. Squeeze film air damping in MEMS. Sensors and Actuators A: Physical, 136(1), 3-27; 2007.
13. Feng C, Zhao YP, Liu DQ. Squeeze-film effects in MEMS devices with perforated plates for small amplitude vibration. Microsystem technologies, 13(7), 625; 2007.
14. Pandey AK, Pratap R. A comparative study of analytical squeeze film damping models in rigid rectangular perforated MEMS structures with experimental results. Microfluidics and Nanofluidics, 4(3), 205-218; 2008.
15. Li P, Fang Y, Xu F. Analytical modeling of squeeze-film damping for perforated circular microplates. Journal of Sound and Vibration, 333(9), 2688-2700; 2014.
16. Tijdeman H. On the propagation of sound waves in cylindrical tubes. Journal of Sound and Vibration, 39(1), 1-33; 1975.
17. Naderyan V, Raspet R, Hickey C, Mohammadi M. Acoustic end correction for micro-perforated plates. In preparation for submission to JASA-EL; 2019.